Journal of Hazardous Materials 183 (2010) 583–589

Contents lists available at ScienceDirect

Journal of Hazardous Materials

journal homepage: www.elsevier.com/locate/jhazmat

Removal of lead from aqueous solution by activated carbon prepared from *Enteromorpha prolifera* by zinc chloride activation

Yanhui Li[a,b,*], Qiuju Du[a], Xiaodong Wang[b], Pan Zhang[a], Dechang Wang[b], Zonghua Wang[a], Yanzhi Xia[a]

[a] *Laboratory of Fiber Materials and Modern Textile, The Growing Base for State Key Laboratory, Qingdao University, 308 Ningxia Road, Qingdao 266071, China*
[b] *College of Electromechanical Engineering, Qingdao University, 308 Ningxia Road, Qingdao 266071, China*

ARTICLE INFO

Article history:
Received 25 May 2010
Received in revised form 12 July 2010
Accepted 12 July 2010
Available online 21 July 2010

Keywords:
Activated carbon
Enteromorpha prolifera
Lead
Activation
Adsorption

ABSTRACT

Activated carbon was prepared from *Enteromorpha prolifera* (EP) by zinc chloride activation. The physico-chemical properties of EP-activated carbon (EPAC) were characterized by thermal stability, zeta potential and Boehm titration methods. The examination showed that EPAC has a porous structure with a high surface area of 1688 m^2/g. Batch adsorption experiments were carried out to study the effect of various parameters such as initial pH, adsorbent dosage, contact time and temperature on Pb(II) ions adsorption properties by EPAC. The kinetic studies showed that the adsorption data followed a pseudo second-order kinetic model. The isotherm analysis indicated that the adsorption data can be represented by Freundlich isotherm model. Thermodynamic studies indicated that the adsorption reaction was a spontaneous and endothermic process.

1. Introduction

The presence of lead ions in the aquatic environment has been of great concern to scientists due to their increased discharge, non-biodegradable, toxic, and other adverse effects on human being as well as the fauna and flora [1]. Many methods such as chemical precipitation [2], electrochemical reduction [3], ion exchange [4], reverse osmosis, and membrane separation [5] have been developed to remove lead from wastewater. However, these technologies are either expensive for the treatment and disposal of the secondary toxic metal sludge or ineffective when lead is present in the wastewater at low concentrations [6]. Currently, activated carbon adsorption is a widely used technology because it is simple, low cost and effective for removing low lead concentration waste streams. The properties such as surface charge, type of surface functional groups, specific surface area, and pore-size distribution affect the adsorption capabilities of metal ions on activated carbon. While all above mentioned physical and chemical properties of activated carbon depend on the precursor materials and activation methods used. So, research interest in the production of activated carbon with high qualities has been focused on two aspects.

One way is to search for suitable precursors. Recently, biomass have attracted increasing attention due to their high efficiency, low operating cost, minimization of chemical sludge, regeneration of biosorbent, and the possibility of metal recovery [7,8]. Activated carbon produced from a variety of biomass of *Tamarind* wood [9], *Polygonum orientale* Linn. [10], hazelnut husks [11], coconut shell [12], palm shell [13], and coffee residue [14] have shown attracting experimental results for lead removal.

Another approach is to explore appropriate activation methods. Generally, two different processes of physical and chemical activations were used to prepare activated carbon [15,16]. Physical activation is to carbonize raw materials at the high temperatures in an inert atmosphere followed by oxidation treatment with steam, air, or CO_2 [17]. Chemical activation involves impregnation of the raw materials with dehydrating chemical agents including phosphoric acid [18], sulfuric acid [14], KOH [19], NaOH [20], and $ZnCl_2$ [21–23]. The advantages of lower temperature and high carbonization yield of the chemical activation make it be widely used to produce activated carbon. $ZnCl_2$ is an effective dehydrating chemical agent. The impregnation with $ZnCl_2$ plays an important role in increasing carbonization ability of the precursors and acquiring a desired pore structure of activated carbon.

EP, one of the widely available marine biomaterials in china [24,25], have proved to be economic, eco-friendly, and effective heavy metal adsorbents due to their special cell wall structures containing functional groups such as amino, hydroxyl, carboxyl and sulphate, which can act as binding sites for metals via both electrostatic attraction and complexation [26–28]. However, to our

* Corresponding author at: Laboratory of Fiber Materials and Modern Textile, The Growing Base for State Key Laboratory, Qingdao University, 308 Ningxia Road, Qingdao 266071, China. Tel.: +86 532 8595 1842; fax: +86 532 8595 1842.
E-mail address: liyanhui@tsinghua.org.cn (Y. Li).

0304-3894/$ – see front matter © 2010 Elsevier B.V. All rights reserved.
doi:10.1016/j.jhazmat.2010.07.063

knowledge, no investigations have been carried on the use of activated carbon from EP as an adsorbent for heavy metal removal.

The purpose of this study aims to develop an effective adsorbent from EP through $ZnCl_2$ activation and investigate its lead removal capability. TGA/DTA analysis was used to characterize the pyrolysis properties of EP. The SEM, Zeta potential, and BET were applied to analyze the physico-chemical properties of EPAC. The effect of various experimental parameters on the lead adsorption process, such as pH, adsorbent dosage, contact time, and temperature were studied.

2. Materials and methods

2.1. Preparation of EPAC

The precursor used for the preparation of the activated carbon was EP, collected from the Yellow Sea coast in Qingdao, China. It was washed several times using tap water to remove impurities and dried in an oven at 100 °C for 24 h until all the moisture evaporated. The dried EP was ground by ball milling (XQM-0.4L) to 120 meshes. The pyrolysis property of EP was carried out at a heating rate of 10 °C/min from 30 to 800 °C in an atmosphere of N_2 at a flow rate of 50 mL/min using a Mettler TGA/STDA 851 thermogravimetric analyzer. 40 g EP was impregnated with $ZnCl_2$ solution containing 40 g of zinc chloride. After 12 h impregnation period, the mixtures were dehydrated at 100 °C for 24 h and then pyrolysed in a quartz tube under N_2 atmosphere at 500 °C for 1 h. EPAC was cooled to room temperature and boiled in a solution of HCl (1 M) for 30 min. Then it was washed with deionized water to remove remained $ZnCl_2$ and HCl. The final product of EPAC was dried at 100 °C for 24 h.

2.2. Characterization of EPAC

The morphology and surface structure of EP and EPAC were examined with JSM 6700F Scanning Microscope. The BET surface area of EPAC was measured from N_2 adsorption isotherm at 77 K using Brunauer–Emmet–Teller equation. The N_2 adsorption isotherm was carried out using Micrometric ASAP 2000 system. Zeta potential of EPAC was measured by a Malvern zetameter (Zetasizer 2000). The values of zeta potential of EPAC were determined through adjusting pH from 2.0 to 8.0 by adding 0.1 M hydrochloric acid or sodium hydroxide solution to the glass beaker at 25 °C. Determination of the quantity of the functional groups on EPAC was conducted using Boehm method [29].

2.3. Batch adsorption experiments

Stock solution of Pb(II) ions (1000 mg/L) was prepared by dissolving the analytical reagent grade lead nitrate (Rgent, Tianjin, China) in deionized water. The stock solution was further diluted to the required concentrations before used. The initial solution pH was adjusted to 5.0 with HNO_3. The concentrations of Pb(II) ions were measured by atomic adsorption spectrometer (Shimadzu model AA-670). Amount of Pb(II) ions adsorbed at equilibrium was calculated using the following equation:

$$q_e = \left(\frac{C_0 - C_e}{m}\right) V \quad (1)$$

where C_0 and C_e were initial and equilibrium concentrations of metal ion (mg/L), respectively, m was the mass of adsorbent (g) and V was volume of the solution (L).

The effect of pH on Pb(II) ion removal was studied by adjusting initial pH from 2.0 to 6.5 using 100 mL of solutions with Pb(II) ion concentrations of 20, 40 and 60 mg/L, respectively. The effect of adsorbent dose on Pb(II) removal was studied by agitating 100 ml of 20, 40 and 60 mg/L solutions of Pb(II) ions containing different dosages of adsorbent (0.02–0.17 mg) for a period of 2 h.

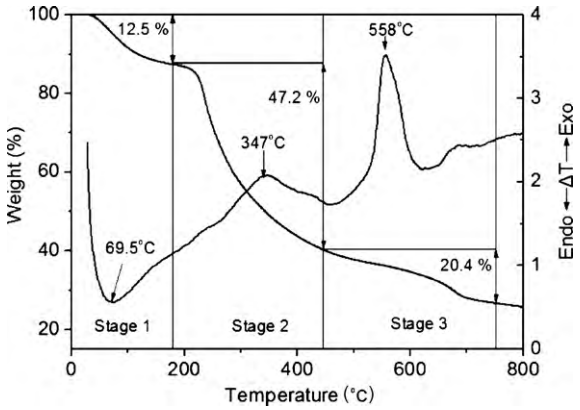

Fig. 1. TGA/DTA profiles of EP (heating rate: 10 °C/min, N_2 flow rate: 50 mL/min).

The effect of agitation time on Pb(II) ion removal was conducted by adding 0.05 g of adsorbents into 100 mL solution with different Pb(II) ion concentrations (20, 40 and 60 mg/L) in 250 mL conical flasks. At predetermined time intervals, samples were collected utilizing a 0.45 mm membrane filter and then analyzed by an atomic adsorption spectrometer. The amounts of Pb(II) ions adsorbed were calculated using the equation (1).

To evaluate the thermodynamic properties, 0.05 g adsorbents were added into 100 mL solutions with pH of 5.0 and initial Pb(II) ion concentrations ranging from 10 to 60 mg/L in a step size of 10 mg/L. These samples were shaken continuously for 2 h at 5, 25, and 35 °C, respectively.

3. Results and discussion

3.1. Characterization of EP and EPAC

3.1.1. Pyrolysis characterization of EP

The TGA/DTA plots (Fig. 1) indicate that the pyrolysis process of EP exhibits three obvious degradation stages. The first stage is a process of dehydration and desiccation to lose the water in the cells and the external water bounded by surface tension [25]. The release of absorbed water in EP leads to a weight loss of 12.5% at temperature range of 30–175 °C and an endothermic peak of 69.5 °C is found in the DTA curve. The significant weight loss appears at the second stage and it reaches 47.6% at the temperature range from 175 to 450 °C. Previous report indicated that chemical constituents of *Enteromorpha* spp. consisted of 9–14% protein, 2–3.6% ether extract, 32–36% ash, and 21% of total fatty acid [30]. The decomposition of proteins, ether extract and fatty acid releases large quantity of heat (exothermic peak of 347 °C) and plays an important role in weight loss in this prolysis process. The third stage is a combustion reaction of organic residues. The exothermic peak caused by combustion appears at 558 °C. The weight loss at this stage is 20.4% [31].

3.1.2. SEM observation

SEM image (Fig. 2a) shows that the surface of the precursor of EP is very smooth and there are very little pores on it. After $ZnCl_2$ impregnation and activation at 500 °C under N_2 atmosphere, the surface of EPAC become rough and many pores appear on it (Fig. 2b). It was reported that $ZnCl_2$ impregnation had important impact on the increase in specific surface area and generation of micropores [23]. The role of $ZnCl_2$ maybe lie in that impregnation of EP with $ZnCl_2$ makes $ZnCl_2$ mix with EP homogeneously, it occupies a volume and inhibits the contraction of the particle during the carbonization, which can leave

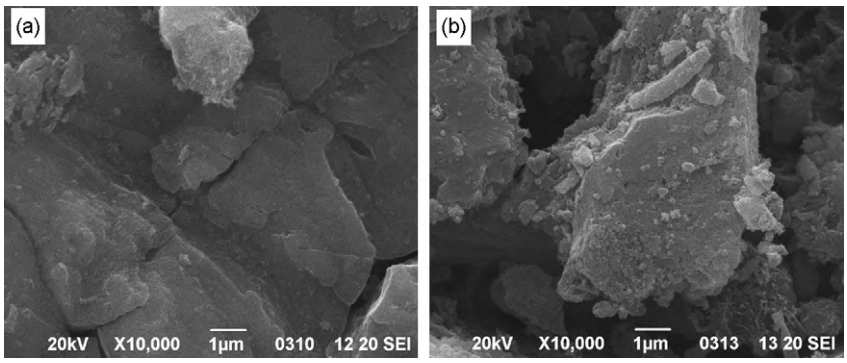

Fig. 2. SEM images of (a) EP and (b) EPAC.

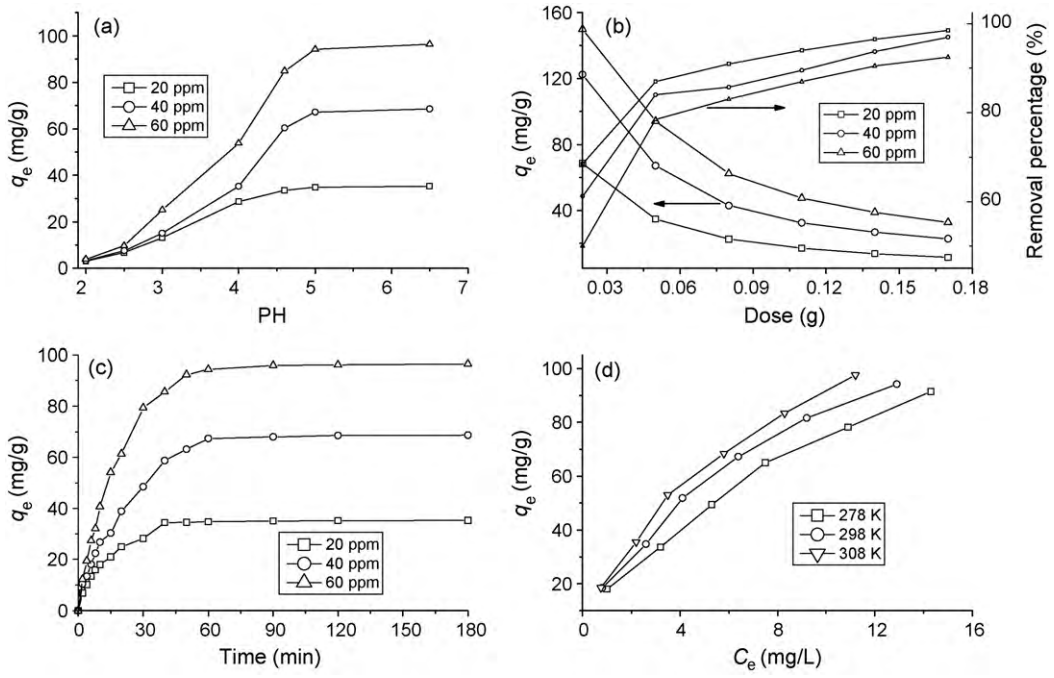

Fig. 3. The effect of the experimental parameters on Pb(II) ion adsorption by EPAC: (a) pH effect (equilibrium time = 2 h, dosage = 0.5 g/L, temperature = 25 °C), (b) dosage effect (pH = 5.0, equilibrium time = 2 h, temperature = 25 °C), (c) contact time effect (pH = 5.0, dosage = 0.5 g/L, temperature = 25 °C), (d) temperature effect (pH = 5.0, equilibrium time = 2 h, dosage = 0.5 g/L).

porosity structure after being washed off with deionized water [32].

3.1.3. Boehm titrations

The quantities of the functional groups on the surface of EPAC were measured by Boehm titration method [29]. The method based on that NaOH titrates carboxyl, lactone and phenolic groups, Na_2CO_3 titrates carboxyl and lactone, and $NaHCO_3$ only titrates carboxyl groups. Based on the known volume of used acid and bases, the different kinds of functional groups can be quantitatively calculated. Table 1 shows that the quantities of carboxyls, phenols, and lactones are 0.97, 0.53 and 1.34 meq/g, respectively (Table 1). The large quantities of the acidic oxygen-containing functional groups on the surface of EPAC make it have high cation exchange capacity and benefit for the heavy metal ion adsorption [33].

Table 1
Physico-chemical properties of EPAC.

Physico-chemical properties	400 (°C)	500 (°C)	600 (°C)	700 (°C)
BET specific surface area (m^2/g)	1416	1688	1398	1392
Pore volume (cm^3/g)[a]	0.90	1.04	0.88	0.84
Pore size (nm)[b]	2.56	2.47	2.51	2.42
Carboxylic functions (meq/g)	N/A	0.97	N/A	N/A
Lactones (meq/g)	N/A	1.34	N/A	N/A
Phenolic functions (meq/g)	N/A	0.53	N/A	N/A
pH_{IEP}	N/A	2.71	N/A	N/A

[a] Single point adsorption total pore volume of pores less than 93.1 nm width at $P/P_0 = 0.98$.
[b] Adsorption average pore width (4 V/A by BET).

3.1.4. Zeta potential measurement

Activated carbon is usually considered as amphoteric solids due to the existence of variety of surface functional groups [34]. Therefore, the isoelectric point (IEP) of EPAC can be evaluated through getting the pH value at which the zeta potential is zero. IEP is used to qualitatively assess the polarity of the adsorbent surface charge [35]. At pH < IEP, the adsorbent has positive surface charge and can act as anion exchanger. While at pH > IEP, the surface charge of the adsorbent is negative, which benefits for adsorbing cations. IEP of EP is 4.43, while it decreases to 2.71 for EPAC (Table 1). This indicates that activation of EP leads to a negatively charged surface of EPAC due to the dissociation of carboxyl functional groups [36].

3.1.5. BET characterization

The specific surface area is a significant factor to affect the adsorption property of activated carbon. Table 1 clearly shows that the specific surface area of EPAC is greatly influenced by the activation temperature. It increases from 1415 to 1688 m^2/g with increasing temperature from 400 to 500 °C. The maximum specific surface area of EPAC maybe attributed to that all organics of proteins, ether extract and fatty acid decompose completely at 500 °C, which leaves a perfect porous structure of EPAC. As temperature increases to 600 or 700 °C, the collapse of the structure of EPAC will lead to the decrease in the specific surface area [37]. A similar trend is observed for the total pore volume calculated from the amount of N_2 adsorbed at relative pressure of $P/P_0 = 0.98$ (Table 1).

3.2. Pb(II) adsorption

3.2.1. Effect of initial pH

The pH of the solution is one of the most important factors to determine the adsorption property of an adsorbent due to its effect not only on surface charge of the adsorbent, but also on the degree of ionisation and speciation of adsorbate [11,12]. The influence of initial solution pH on Pb(II) ion removal by EPAC is shown in Fig. 3a. At pH 2.0, the competition of H^+ and Pb(II) ions for the same adsorption active sites [33] leads to the lower Pb(II) ion adsorption capacity of EPAC. On the other hand, EPAC has the positive surface charge (IEP = 2.71) at pH 2.0 and it repels cations due to the electrostatic force of repulsion. As pH > 2.71, the amount of Pb^{2+} adsorbed by EPAC increases rapidly with increasing of the density of negative charge on the adsorbent surfaces due to ionization of COOH groups and negative charge present in EPAC [33]. At pH = 5.0, the adsorption capacity of EPAC almost reaches the maximum value at different initial Pb(II) ion concentrations. Because the speciation diagram of lead shows that at pH > 6.0 the species such as $[Pb(OH)]^+$, $[Pb_3(OH)_4]^+$, and $[Pb(OH)_2]$ will be produced [38], in order to guarantee to truly examine the adsorption property of EPAC as well as to avoid precipitation of Pb(II) ions, all the following experiments were conducted at pH 5.0.

3.2.2. Effect of adsorbent dosage

Fig. 3b shows the effect of adsorbent dosage on Pb(II) ion removal percentage and adsorption capacity of EPAC. It is clear that the Pb(II) ion removal percentage increases sharply with increasing EPAC dose from 0.02 to 0.05 g. This may be due to the greater adsorbent surface area and pore volume available at higher adsorbent dosage providing more functional groups and active adsorption sites that results in a higher Pb(II) ion removal percentage [39]. As further increase in adsorbent dosage from 0.08 to 0.17 g, the Pb(II) ion removal percentage gradually increases to 98.52, 97.11 and 92.21%, respectively, for initial Pb(II) ion concentrations of 20, 40 and 60 mg/L at the EPAC dose of 0.17 g. The figure also indicates that the Pb(II) ion equilibrium adsorption capacity of EPAC decreases with increasing EPAC dose. It is due to that all active sites are entirely exposed and utilized at lower EPAC dose. With increasing of EPAC dose, only part of active sites are exposed and occupied by Pb(II) ions, leading to a lower adsorption capacity [1]. At the same EPAC dosage, higher Pb(II) ion concentration increases the diffusion driving force of Pb(II) ions adsorbed by EPAC due to the larger Pb(II) ion concentration gradient [40] and thus acquires a higher equilibrium adsorption capacity.

3.2.3. Effect of contact time

The effect of contact time on Pb(II) ions adsorbed by EPAC was studied and shown in Fig. 3c. It can be seen that the adsorption of Pb(II) ions is rapid during the first 20 min and the Pb(II) ion adsorption capacity of EPAC increases with the initial Pb(II) ion concentration. The fast adsorption at the initial stage may be due to the higher driving force making fast transfer of metal ions to the surface of adsorbent particles and the availability of the uncovered surface area and the active sites on the adsorbent [41,42]. With further increasing time, the availability of the uncovered surface area and the remaining active sites diminishes and the decrease in the driving force make it take long time to reach equilibrium for metal ions slowly diffusing into the intra-particle pores of the adsorbent [41]. Thus, the adsorption rate becomes slower. It takes about 40 min to reach adsorption equilibrium for EPAC at initial Pb(II) ion concentration of 20 mg/L. With increasing of initial Pb(II) ion concentration, the equilibrium time increases further. Similar result in Pb(II) ion removal by activated carbon has been reported in Ref. [12].

3.2.4. Effect of temperature

The temperature has two main effects on the adsorption processes of the porous adsorbents. It can affect the diffusion rate of the sorbate within the pores as a result of decreasing solution viscosity [23] and the number of the sorption sites generated because of breaking of some internal bonds near the edge of active surface sites of sorbent [43], which benefits for improving the adsorption capacity of the adsorbents. Fig. 3d shows that the adsorption capacity of Pb(II) ions adsorbed by EPAC increases with the increase in temperature. The adsorption capacity increases from 75.52 to 91.54 mg/g at Pb(II) ion equilibrium concentration of 10 mg/L as the temperature rises from 5 to 35 °C. The results indicate that the adsorption reaction of Pb(II) ions adsorbed by EPAC is endothermic process, i.e. increasing temperature can increase the diffusion rate of Pb(II) ions and the number of the sorption sites and thus enhance the adsorption ability of EPAC.

3.3. Adsorption isotherms

The Freundlich and Langmuir models are the most frequently used models to describe the experimental data of adsorption isotherms. Here, both models were used to investigate how Pb(II) ions interact with adsorbents, the Langmuir and Freundlich models were applied to describe the isotherm data obtained at three temperatures.

The Freundlich isotherm is an empirical equation based on an exponential distribution of adsorption sites and energies. It is represented as

$$\mathrm{Ln}\, q_e = \mathrm{Ln}\, k_F + \frac{1}{n}\mathrm{Ln}\, c_e \quad (2)$$

where k_F (L/g) and n are Freundlich constants related to adsorption capacity and adsorption intensity, respectively. From the slope and intercept of straight portion of the linear plot obtained by plotting $\mathrm{Ln}\, q_e$ against $\mathrm{Ln}\, C_e$, the values of Freundlich parameters were calculated and listed in Table 2. The correlation coefficients r^2 (Table 2) suggest that the isotherm data fit the Freundlich model well. The high values of k_F indicate that EPAC has a higher adsorption capacity and affinity for Pb(II) ions.

Table 2
Parameters of Freundlich and Langmuir adsorption isotherm models for Pb(II) ions adsorbed by EPAC.

Temperature (°C)	Freundlich			Langmuir		
	n	k_F	r^2	q_{max}	k_L	r^2
5	1.60	17.47	0.9949	142.93	0.11	0.9662
25	1.65	20.92	0.9937	146.85	0.15	0.9746
35	1.61	22.50	0.9953	147.06	0.16	0.9853

The Langmuir isotherm assumes a surface with homogeneous binding sites, equivalent sorption energies, and no interaction between adsorbed species. Its mathematical form is written as:

$$\frac{C_e}{q_e} = \frac{C_e}{q_{max}} + \frac{1}{q_{max} k_L} \quad (3)$$

where q_{max} and k_L represent the maximum adsorption capacity for the solid phase loading and the energy constant related to the heat of adsorption respectively. A straight line is obtained when C_e/q_e was plotted against C_e and q_{max} and k_L could be calculated from the slopes and intercepts (Table 2). Although the correlation coefficients r^2 (0.9662, 09746 and 0.9853) of the Langmuir equation are lower than those of the Freundlich equation, the Langmuir equation can be used to roughly evaluate the Pb(II) ion maximum adsorption capacity of EPAC. The Pb(II) ion maximum adsorption capacity of EPAC is listed in Table 2 and compared with activated carbon prepared from other precursors (Table 3). The comparison shows that EPAC has high Pb(II) ion adsorption capacity of 146.85 mg/g, suggesting that it is a promising adsorbent to remove heavy metals from aqueous solutions.

3.4. Kinetic studies

In order to investigate the controlling mechanism of adsorption processes, the pseudo first-order and pseudo second-order rate equation [23] were applied to analyze the kinetic adsorption data obtained at three different initial Pb(II) ion concentrations.

The linearized-integral form of the pseudo first-order model is expressed as follows:

$$\log(q_e - q_t) = \log q_e - \frac{k_1}{2.303} t \quad (4)$$

where k_1 is the Lagergren rate constant of adsorption (1/min), The values of q_e (25.48, 74.20, and 85.59 mg/g) and k_1 (0.07, 0.05 and 0.05 1/min) at initial Pb(II) ion concentrations of 20, 40 and 60 mg/L, respectively are determined from the plot of $\log(q_e - q_t)$ against t. While the lower correlation coefficients r^2 (0.9200, 0.9808, and 0.9701) suggest that adsorption of Pb(II) ion by EPAC does not follow the pseudo first-order kinetic. The unfittingness of the pseudo first-order kinetic model may be due to a boundary layer controlling the beginning of the adsorption process [23].

The linearized-integral form of the pseudo second-order model is:

$$\frac{t}{q_t} = \frac{1}{k_2 q_e^2} + \frac{t}{q_e} \quad (5)$$

where k_2 is the pseudo second-order rate constant of adsorption (g/mg min).

From the slopes and intercepts of straight portion of the linear plots obtained by plotting t/q_t vs. t, the values of the pseudo second-order rate constants q_e and k_2 were calculated. The higher correlation coefficients, r^2, of the pseudo-second-order rate model are 0.9971, 0.9928, and 0.9943, respectively for the initial Pb(II) ion concentrations of 20, 40, and 60 mg/mL, suggesting that the kinetic modeling of the Pb(II) ions adsorbed by EPAC well follows the pseudo second-order rate model. This means that the overall rate of Pb(II) ion adsorption process seems to be controlled by the chemical process through sharing of electrons or by covalent forces through exchanging of electrons between adsorbent and adsorbate [45].

3.5. Adsorption mechanism

For a solid liquid adsorption process, to analyze the rate controlling steps such as mass transport and chemical reaction processes is very beneficial for elaborating the adsorption mechanism. The adsorption reaction is usually divided into the following steps [27,46]:

1. Metal ion from the bulk liquid to the liquid film or boundary layer surrounding the adsorbent.
2. Transport of solute ions from the boundary film to the external surface of the biosorbent (film diffusion).
3. Transfer of ions from the surface to the intra-particular active sites (particle diffusion).
4. Adsorption of ions by the active sites of adsorbent.

Because the first step is not involved with adsorbent and the fourth step is a very rapid process, they do not belong to the rate controlling steps. Therefore, the rate controlling steps mainly depend on either film diffusion or particle diffusion.

Weber and Morris model is a widely used intra-particle diffusion model to predict the rate controlling step [10,47]. The rate constants

Table 3
Adsorption capacities of Pb(II) ions by various adsorbents.

Activated carbon source	Experimental conditions					Refs.
	Dosage (g/L)	pH	Temp. (°C)	Concentration (mg/L)	q_{max} (mg/g)	
Euphorbia rigida	3.0	6.5	25	40	134.22	[9]
Polygonum orientale Linn.	0.6	5.0	25	50–75	98.39	[10]
Hazelnut husks	12.0	5.7	25	200	13.05	[11]
Palm shell	5.0	5.0	27	10–700	95.2	[13]
Cattle manure compost	0.6	5.5	25	50	8.65	[16]
Coconut shell	2.0	3.2–3.6	25	20–260	40.12	[34]
Palm shell	2.5	5.0		40–120	82.46	[42]
Tamarind wood	2.0	5.68	30	10–50	43.85	[43]
Sugar cane husk		5.0	25	5–120	8.58	[44]
EPAC	0.5	5.0	25	10–60	146.85	This study

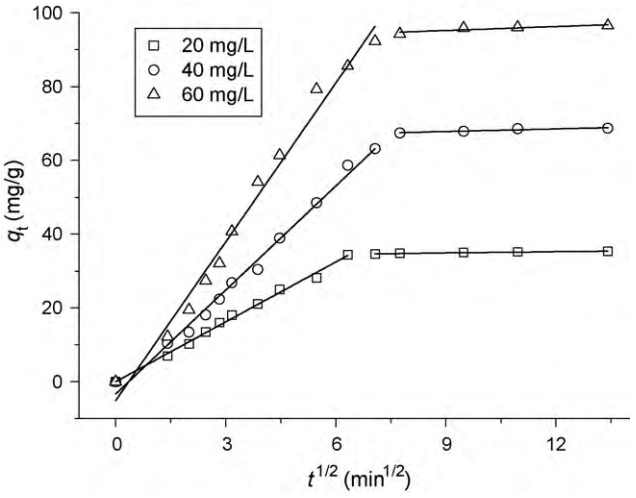

Fig. 4. Intra-particle diffusion model for the adsorption of Pb(II) ion onto EPAC.

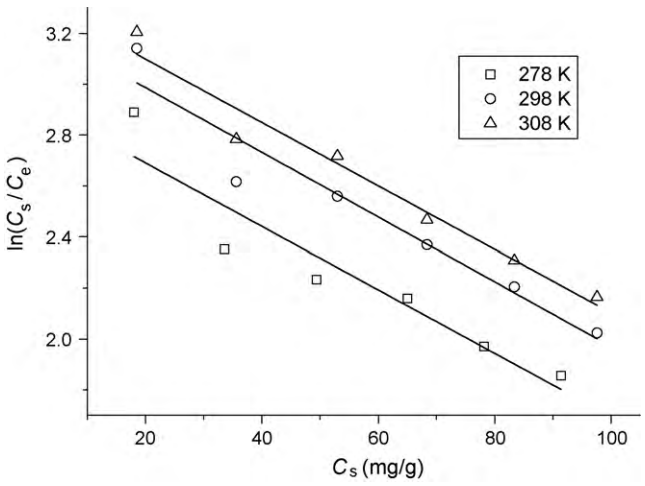

Fig. 5. Plots of ln C_s/C_e vs. C_s for calculation of thermodynamic parameters.

of intra-particle diffusion (k_{id}) at the stage *i* were determined using the following equation:

$$q_t = k_{id} t^{1/2} + C_i \quad (6)$$

where q_t is the amount adsorbed Pb(II) ion at time *t*, $t^{1/2}$ is the square root of the time, C_i is the intercept at stage *i*. The value of C_i is related to the thickness of the boundary layer. The plots of q_t vs. $t^{1/2}$ at different initial Pb(II) ion concentrations show multi-linearity characterizations (Fig. 4), indicating that two steps occurred in the adsorption process [48]. The first sharp section is the external surface adsorption or instantaneous adsorption stage. The second subdued portion is the gradual adsorption stage, where intra-particle diffusion is rate-controlled [49]. The larger slopes of the first sharp sections indicate that the rate of metal removal is higher in the beginning stage due to the instantaneous availability of large surface area and active adsorption sites. The lower slopes of the second subdued portion are due to that the decreased concentration gradients make Pb(II) ion diffusion in the micropores of adsorbent take long time, thus leading to a low removal rate. The obvious two steps of the plots as well as their deviation from the origin suggests that the intra-particle diffusion is not the only rate controlling step for the adsorption of Pb(II) ions onto EPAC [50].

3.6. Thermodynamic study

Thermodynamic parameters can be calculated from the variation of the thermodynamic equilibrium constant K_0 with the change in temperature [51]. For adsorption reactions, K_0 is defined as follows:

$$K_0 = \frac{a_s}{a_e} = \frac{v_s}{v_e}\frac{C_s}{C_e} \quad (7)$$

where a_s is the activity of adsorbed Pb(II) ions, a_e is the activity of the Pb(II) ions in solution at equilibrium, C_s is the amount of Pb(II) ions adsorbed by per mass of EPAC, v_s is the activity coefficient of the adsorbed Pb(II) ions and v_e is the activity coefficient of the Pb(II) ions in solution. As the Pb(II) ion concentration in the solution decreases and approaches to zero, K_0 can be obtained by plotting $\ln(C_s/C_e)$ vs. C_s and extrapolating C_s to zero (Fig. 5) [51]. The straight line obtained is well fitted to the points based on a least-squares analysis and its intercept with the vertical axis gives the values of K_0.

The adsorption standard free energy changes (ΔG^0) can be calculated according to:

$$\Delta G^0 = -RT \ln K_0 \quad (8)$$

Table 4
Values of various thermodynamic parameters for adsorption of Pb(II) ions adsorbed by EPAC.

Thermodynamic constant	Temperature (K)		
	278	298	308
K_0	2.94	3.24	3.35
ΔG_0 (cal/mol)	−595.70	−696.09	−739.88
ΔH^0 (cal/mol)	741.15	741.15	741.15
ΔS^0 (cal/mol K)	4.81	4.82	4.81

where *R* is the universal gas constant (1.987 cal/° mol) and *T* is the temperature in Kelvin.

The average standard enthalpy change (ΔH^0) is obtained from Van't Hoof equation:

$$\ln K_0(T_3) - \ln K_0(T_1) = \frac{-\Delta H^0}{R}\left(\frac{1}{T_3} - \frac{1}{T_1}\right) \quad (9)$$

where T_3 and T_1 are two different temperatures. The standard entropy change (ΔS^0) can be obtained by:

$$\Delta S^0 = -\frac{\Delta G^0 - \Delta H^0}{T} \quad (10)$$

The thermodynamic parameters were listed in Table 4. Positive values of ΔH^0 suggests that the interaction of Pb(II) ions adsorbed by EPAC is endothermic process, which supported by the increasing adsorption of Pb(II) ions with the increase in temperature. The negative values of ΔG^0 revealed the fact that adsorption process was spontaneous. The positive value of ΔS^0 indicates increased randomness at the adsorbent/solution interface during the adsorption of Pb(II) ions onto EPAC [45].

4. Conclusions

Activated carbon with high Pb(II) ion adsorption capacity was prepared from EP by zinc chloride activation at 500 °C. The physicochemical characterization of EPAC shows that EPAC has a large specific surface area of 1688 m^2/g and a IEP of 2.71. Boehm titration study shows that there are large quantity of the functional groups such as carboxylic, hydroxyl, and phenolic groups existed on the surfaces of EPAC. Batch adsorption experiments show that Pb(II) ion adsorption properties of EPAC are great dependent on pH, adsorbent dosage, and temperature. The kinetics studies show that the experimental data can be well fitted by the pseudo second-order rate equation. The adsorption of Pb(II) ion is very rapid in the initial stage and decreases while approaching equilibrium, suggesting that the intra-particle diffusion is not the only rate controlling step

for the adsorption of Pb(II) ions onto EPAC. The adsorption equilibrium is well described by the Freundlich adsorption isotherm. Thermodynamic studies indicate an endothermic nature and a spontaneous process for the Pb(II) ion adsorbed by EPAC.

Acknowledgements

This work was supported by the National Natural Science Foundation of China (50802045 and 20975056/B050902) SRF for ROCS, SEM, the Middle-aged and Youth Scientist Incentive Foundation of Shandong Province (BS09018) and the Taishan Scholar Program of Shandong Province, China.

References

[1] V.K. Gupta, A. Rastogi, Biosorption of lead from aqueous solutions by green algae *Spirogyra* species: kinetics and equilibrium studies, J. Hazard. Mater. 152 (2008) 407–414.
[2] Z. Djedidi, M. Bouda, M.A. Souissi, R.B. Cheikh, G. Mercier, R.D. Tyagi, J.F. Blais, Metals removal from soil, fly ash and sewage sludge leachates by precipitation and dewatering properties of the generated sludge, J. Hazard. Mater. 172 (2009) 1372–1382.
[3] S.W. Lin, R.M.F. Navarro, An innovative method for removing Hg^{2+} and Pb^{2+} in ppm concentrations from aqueous media, Chemosphere 39 (1999) 1809–1817.
[4] M. Islam, R. Patel, Removal of lead(II) from aqueous environment by a fibrous ion exchanger: polycinnamamide thorium(IV) phosphate, J. Hazard. Mater. 172 (2009) 707–715.
[5] D.W. O'Connell, C. Birkinshaw, T.F. O'Dwyer, Heavy metal adsorbents prepared from the modification of cellulose: a review, Bioresour. Technol. 99 (2008) 6709–6724.
[6] Z.Y. He, H.L. Nie, C. Branford-White, L.M. Zhu, Y.T. Zhou, Y. Zheng, Removal of Cu^{2+} from aqueous solution by adsorption onto a novel activated nylon-based membrane, Bioresour. Technol. 99 (2008) 7954–7958.
[7] K. Vijayaraghavan, K. Palanivelu, M. Velan, Biosorption of copper(II) and cobalt(II) from aqueous solutions by crab shell particles, Bioresour. Technol. 97 (2006) 1411–1419.
[8] V.J.P. Vilar, C.M.S. Botelho, R.A.R. Boaventura, Lead and copper biosorption by marine red algae Gelidium and algal composite material in a CSTR ("Carberry" type), Chem. Eng. J. 138 (2008) 249–257.
[9] C.K. Singh, J.N. Sahu, K.K. Mahalik, C.R. Mohanty, B. Raj Mohan, B.C. Meikap, Studies on the removal of Pb(II) from wastewater by activated carbon developed from Tamarind wood activated with sulphuric acid, J. Hazard. Mater. 153 (2008) 221–228.
[10] L. Wang, J. Zhang, R. Zhao, Y. Li, C. Li, C. Zhang, Adsorption of Pb(II) on activated carbon prepared from *Polygonum orientale* Linn.: kinetics, isotherms, pH, and ionic strength studies, Bioresour. Technol. 101 (2010) 5808–5814.
[11] M. Imamoglu, O. Tekir, Removal of copper(II) and lead(II) ions from aqueous solutions by adsorption on activated carbon from a new precursor hazelnut husks, Desalination 228 (2008) 108–113.
[12] M. Sekar, V. Sakthi, S. Rengaraj, Kinetics and equilibrium adsorption study of lead(II) onto activated carbon prepared from coconut shell, J. Colloid Interface Sci. 279 (2004) 307–313.
[13] G. Issabayeva, M.K. Aroua, N.M.N. Sulaiman, Removal of lead from aqueous solutions on palm shell activated carbon, Bioresour. Technol. 97 (2006) 2350–2355.
[14] S. Karagöz, T. Tay, S. Ucar, M. Erdem, Activated carbons from waste biomass by sulfuric acid activation and their use on methylene blue adsorption, Bioresour. Technol. 99 (2008) 6214–6222.
[15] J. Acharya, J.N. Sahu, B.K. Sahoo, C.R. Mohanty, B.C. Meikap, Removal of chromium(VI) from wastewater by activated carbon developed from Tamarind wood activated with zinc chloride, Chem. Eng. J. 150 (2009) 25–39.
[16] M.A.A. Zaini, R. Okayama, M. Machida, Adsorption of aqueous metal ions on cattle-manure-compost based activated carbons, J. Hazard. Mater. 170 (2009) 1119–1124.
[17] Ö. Gerçel, A. Özcan, A.S. Özcan, H. Ferdi Gerçel, Preparation of activated carbon from a renewable bio-plant of *Euphorbia rigida* by H_2SO_4 activation and its adsorption behavior in aqueous solutions, Appl. Surf. Sci. 253 (2007) 4843–4852.
[18] S. Zuo, J. Liu, J. Yang, X. Cai, Effects of the crystallinity of lignocellulosic material on the porosity of phosphoric acid-activated carbon, Carbon 47 (2009) 3574–3584.
[19] A.H. Basta, V. Fierro, H. El-Saied, A. Celzard, 2-Steps KOH activation of rice straw: an efficient method for preparing high-performance activated carbons, Bioresour. Technol. 100 (2009) 3941–3947.
[20] E. Schröder, K. Thomauske, C. Weber, A. Hornung, V. Tumiatti, Experiments on the generation of activated carbon from biomass, J. Anal. Appl. Pyrolysis 79 (2007) 106–111.
[21] T. Wang, S. Tan, C. Liang, Preparation and characterization of activated carbon from wood via microwave-induced $ZnCl_2$ activation, Carbon 47 (2009) 1867–1885.
[22] M. Asadullah, M. Asaduzzaman, M.S. Kabir, M.G. Mostofa, T. Miyazawa, Chemical and structural evaluation of activated carbon prepared from jute sticks for Brilliant Green dye removal from aqueous solution, J. Hazard. Mater. 174 (2010) 437–443.
[23] F. Boudrahem, F. Aissani-Benissad, H. Aït-Amar, Batch sorption dynamics and equilibrium for the removal of lead ions from aqueous phase using activated carbon developed from coffee residue activated with zinc chloride, J. Environ. Manage. 90 (2009) 3031–3039.
[24] D. Liu, J.K. Keesing, Q. Xing, P. Shi, World's largest macroalgal bloom caused by expansion of seaweed aquaculture in China, Mar. Pollut. Bull. 58 (2009) 888–895.
[25] D. Li, L. Chen, J. Zhao, X. Zhang, Q. Wang, H. Wang, N. Ye, Evaluation of the pyrolytic and kinetic characteristics of *Enteromorpha prolifera* as a source of renewable bio-fuel from the Yellow Sea of China, Chem. Eng. Res. Des. 88 (2010) 647–652.
[26] A. Özer, G. Gürbüz, A. Çalimli, B.K. Körbahti, Investigation of nickel(II) biosorption on *Enteromorpha prolifera*: optimization using response surface analysis, J. Hazard. Mater. 152 (2008) 778–788.
[27] A. Özer, G. Gürbüz, A. Çalimli, B.K. Körbahti, Biosorption of copper(II) ions on *Enteromorpha prolifera*: application of response surface methodology (RSM), Chem. Eng. J. 146 (2009) 377–387.
[28] A. Sari, M. Tuzen, Biosorption of cadmium(II) from aqueous solution by red algae (*Ceramium virgatum*): equilibrium, kinetic and thermodynamic studies, J. Hazard. Mater. 157 (2008) 448–454.
[29] H.P. Boehm, Some aspects of the surface chemistry of carbon blacks and other carbons, Carbon 32 (1994) 759–769.
[30] M. Aguilera-Morales, M. Casas-Valdez, S. Carrillo-Dominguez, B. Gonzalez-Acosta, F. Perez-Gil, Chemical composition and microbiological assays of marine algae *Enteromorpha* spp. as a potential food source, J. Food Compos. Anal. 18 (2005) 79–88.
[31] S. Wang, X.M. Jiang, X.X. Han, J.G. Liu, Combustion characteristics of seaweed biomass. 1. Combustion characteristics of *Enteromorpha clathrata* and *Sargassum natans*, Energy Fuels 23 (2009) 5173–5178.
[32] M.A. Díaz-Díez, V. Gómez-Serrano, C. Fernández González, Porous texture of activated carbons prepared by phosphoric acid activation of woods, Appl. Surf. Sci. 238 (2004) 309–313.
[33] P. Miretzky, C. Muñoz, A. Carrillo-Chávez, Experimental binding of lead to a low cost on biosorbent: Nopal (*Opuntia streptacantha*), Bioresour. Technol. 99 (2008) 1211–1217.
[34] X. Song, H. Liu, L. Cheng, Y. Qu, Surface modification of coconut-based activated carbon by liquid-phase oxidation and its effects on lead ion adsorption, Desalination 255 (2010) 78–83.
[35] Y.H. Li, S. Wang, A. Cao, D. Zhao, X. Zhang, C. Xu, Z. Luan, D. Ruan, J. Liang, D. Wu, B. Wei, Adsorption of fluoride from water by amorphous alumina supported on carbon nanotubes, Chem. Phys. Lett. 350 (2001)412–416.
[36] D.J. Malik, V. Strelko Jr., M. Streat, A.M. Puziy, Characterisation of novel modified active carbons and marine algal biomass for the selective adsorption of lead, Water Res. 36 (2002) 1527–1538.
[37] J.W. Kim, M.H. Sohn, D.S. Kim, S.M. Sohn, Y.S. Kwon, Production of granular activated carbon from waste walnut shell and its adsorption characteristics for Cu^{2+} ion, J Hazard Mater. 85 (2001) 301–315.
[38] M. Machida, Y. Kikuchi, M. Aikawa, H. Tatsumoto, Kinetics of adsorption and desorption of Pb(II) in aqueous solution on activated carbon by two-site adsorption model, Colloids Surf. A 240 (2004) 179–186.
[39] Y.H. Li, Z. Luan, X. Xiao, C. Xu, D. Wu, B. Wei, Removal of Cu^{2+} ions from aqueous solutions by carbon nanotubes, Adsorpt. Sci. Technol. 21 (2003)475–485.
[40] S.S. Baral, N. Das, G.R. Chaudhury, S.N. Das, A preliminary study on the adsorptive removal of Cr(VI) using seaweed, *Hydrilla verticillata*, J. Hazard. Mater. 171 (2009) 358–369.
[41] Y. Wu, S. Zhang, X. Guo, H. Huang, Adsorption of chromium(III) on lignin, Bioresour. Technol. 99 (2008) 7709–7715.
[42] M.K. Aroua, S.P.P. Leong, L.Y. Teo, C.Y. Yin, W.M.A.W. Daud, Real-time determination of kinetics of adsorption of lead(II) onto palm shell-based activated carbon using ion selective electrode, Bioresour. Technol. 99 (2008) 5786–5792.
[43] J. Acharya, J.N. Sahu, C.R. Mohanty, B.C. Meikap, Removal of lead(II) from wastewater by activated carbon developed from Tamarind wood by zinc chloride activation, Chem. Eng. J. 149 (2009) 249–262.
[44] L. Giraldo-Gutiérrez, J.C. Moreno-Piraján, Pb(II) and Cr(VI) adsorption from aqueous solution on activated carbons obtained from sugar cane husk and sawdust, J. Sanit. Eng. Div. ASCE 81 (2008) 278–284.
[45] Y. Nuhoglu, E. Malkoc, Thermodynamic and kinetic studies for environmentaly friendly Ni(II) biosorption using waste pomace of olive oil factory, Bioresour. Technol. 100 (2009) 2375–2380.
[46] M. Sarkar, P.K. Acharya, B. Bhattacharya, Modeling the adsorption kinetics of some priority organic pollutants in water from diffusion and activation energy parameters, J. Colloid Interface Sci. 266 (2003) 28–32.
[47] W.J. Weber, J.C. Morriss, Kinetics of adsorption on carbon from solution, J. Sanit. Eng. Div. Am. Soc. Civil Eng. 89 (1963) 31–60.
[48] F.C. Wu, R.L. Tseng, R.S. Juang, Comparisons of porous and adsorption properties of carbons activated by steam and KOH, J. Colloid Interface Sci. 283 (2005) 49–56.
[49] W.H. Cheung, Y.S. Szeto, G. McKay, Intraparticle diffusion processes during acid dye adsorption onto chitosan, Bioresour. Technol. 98 (2007)2897–2904.
[50] Ö. Gerçel, H.F. Gerçel, Adsorption of lead(II) ions from aqueous solutions by activated carbon prepared from biomass plant material of *Euphorbia rigida*, Chem. Eng. J. 132 (2007) 289–297.
[51] Y.H. Li, Z. Di, J. Ding, D. Wu, Z. Luan, Y. Zhu, Adsorption thermodynamic, kinetic and desorption studies of Pb^{2+} on carbon nanotubes, Water Res. 39 (2005) 605–609.